*Can. J. Remote Sensing*, Vol. 33, No. 3, pp. 176–188, 2007

# Evaluation of empirical and semi-empirical backscattering models for surface soil moisture estimation

J. Álvarez-Mozos, M. González-Audícana, and J. Casalí

**Abstract.** Several empirical and semi-empirical backscattering models have been proposed to offer alternative expressions for the inversion of surface parameters from radar data, but the applicability and adequacy of the models for different surface conditions and sensor configurations have not been clearly assessed. A number of empirical and semi-empirical models are studied in this paper to assess the applicability of the models for different conditions that are often found over agricultural areas. The performance of the models is evaluated first analytically by comparing their simulations with those obtained using the theoretical integral equation model (IEM) and geometrical optics model (GOM). The model estimations are then compared with RADARSAT-1 observations acquired over an experimental catchment. The results show very different model behaviour depending on the surfaces roughness conditions and incidence angle. This study highlights the importance of carefully selecting the backscattering model to be used in radar applications.

**Résumé.** Plusieurs modèles empiriques et semi-empiriques de rétrodiffusion ont été proposés pour offrir des expressions alternatives à l'inversion des paramètres de surface à partir des données radar. Cependant, l'applicabilité et la pertinence des modèles aux différentes conditions de surface et configurations de capteurs n'ont pas été évaluées de façon satisfaisante. Dans cet article, nous étudions un nombre de modèles empiriques et semi-empiriques en vue d'évaluer leur applicabilité aux diverses conditions souvent observées en milieu agricole. La performance des modèles est évaluée tout d'abord de façon analytique, c'est-à-dire en comparant leurs simulations avec celles obtenues avec les modèles théoriques IEM (« integral equation model ») et GOM (« geometrical optics model »). Ensuite, les estimations des modèles sont comparées avec des observations RADARSAT-1 acquises au-dessus d'un bassin versant expérimental. Les résultats montrent un comportement très différent des modèles selon les conditions de rugosité de surface et l'angle d'incidence. Cette étude souligne l'importance de bien sélectionner le modèle de rétrodiffusion à utiliser dans les applications radar.
[Traduit par la Rédaction]

## Introduction

Surface soil moisture (SM) is a variable that plays a crucial role in many processes occurring at the soil–atmosphere interface. The knowledge of the moisture content of the soil over a field or a catchment can be very helpful for hydrological, agronomic, and meteorological applications (Schmugge et al., 2002; Moran et al., 2004). However, soil moisture characterization is a complicated task due to its high spatial and temporal variability (Wilson et al., 2004). In addition, most soil moisture measuring devices developed so far consist of point-based probes. Therefore, estimating the moisture content of fields or larger areas by means of remote sensing observations is at present an attractive challenge.

Soil moisture sensing can best be approached using either passive or active microwave sensors (Du et al., 2000; Schmugge et al., 2002). However, passive sensors have a very coarse spatial resolution and are thus limited to small-scale applications. Consequently, active microwave (radar) sensors represent the best alternative for hydrological and agronomic applications. The backscattering coefficient, $\sigma^0$, obtained from radar sensors is directly related to the dielectric properties of the soil surface being observed, which in turn are mainly dependent on its moisture content (Ulaby et al., 1986).

Radar-based SM retrieval has been intensively studied in the last decades. Three main approaches have been generally followed (Moran et al., 2004): (*i*) empirical linear regression models relating the backscattering coefficient to SM which are valid for invariant roughness, vegetation, and scene-acquisition conditions (Glenn and Carr, 2004; Álvarez-Mozos et al., 2005); (*ii*) change detection techniques for monitoring SM dynamics, assuming that surface roughness and vegetation cover change more slowly than does SM (Wickel et al., 2001); and (*iii*) electromagnetic scattering models that simulate the surface backscattering process and can be inverted to retrieve SM (Ulaby et al., 1986; Fung, 1994). The first two approaches have limited validity because they require the surface characteristics apart from SM to remain unchanged and the sensor parameters to be exactly the same. If identical sensor parameters were needed, the revisit time of most sensors would be on the order of several weeks, which is generally insufficient for most

Received 22 May 2006. Accepted 22 March 2007. Published on the *Canadian Journal of Remote Sensing* Web site at http://pubs.nrc-cnrc.gc.ca/cjrs on 18 July 2007.

**J. Álvarez-Mozos,[1] M. González-Audícana, and J. Casalí.** Department of Projects and Rural Engineering, Public University of Navarre, Arrosadia s/n, 31006 Pamplona, Spain.

[1]Corresponding author (e-mail: jesus.alvarez@unavarra.es).

 

hydrological and agronomic applications. Apart from that, vegetation and surface roughness can change dramatically over short time periods in agricultural areas. Therefore, it would seem that the application of electromagnetic scattering models is the most suitable approach for the estimation of SM for hydrological and agronomic applications over agricultural areas; however, this approach requires additional parameters, such as roughness, for each image acquisition.

Several models have been proposed for bare soils or sparsely vegetated surfaces. At present, the integral equation model (IEM) (Fung, 1994) and the geometrical optics model (GOM) (Ulaby et al., 1986) are the recommended and most frequently used algorithms for soil moisture retrieval (Su et al., 1997; Sano et al., 1998; Baghdadi et al., 2002a; Satalino et al., 2002; Mattia et al., 2006). Both are physically based models. The former is applicable to smooth or medium roughness conditions, and the latter to rough or very rough surfaces. Consequently, both models cover the range of roughness conditions that can be expected over most agricultural surfaces. In addition, these theoretical models have been validated against observations acquired on experimental plots or laboratory settings, verifying the adequacy of their predictions as long as their applicability conditions are met (Fung, 1994; Mancini et al., 1999; Macelloni et al., 2000).

The application of the IEM to natural conditions has so far been problematic, however (Altese et al., 1996; Su et al., 1997; Baghdadi et al., 2002b; Baghdadi and Zribi, 2006). The surface roughness description implemented in the model requires three roughness parameters (namely the standard deviation of surface heights, $s$; the surface correlation length, $l$; and the shape of the autocorrelation function, ACF); as a result, the inversion of the soil moisture is markedly complicated at least in the case of single-configuration observations, often leading to an ill-posed problem (Shi et al., 1997; Leconte et al., 2004; Loew and Mauser, 2006; Mattia et al., 2006). Furthermore, it has been reported that an accurate field measurement of the required roughness parameters, in particular $l$, is extremely difficult to perform (Oh and Kay, 1998; Davidson et al., 2000; Baghdadi et al., 2002b).

To overcome these limitations, many researchers highlighted the necessity of multiconfiguration observations that would substantially reduce the number of unknown variables and therefore the dependency on roughness measurements (Bindlish and Barros, 2000; McNairn and Brisco, 2004; Sahebi et al., 2002). Others resorted to the inclusion of a priori information on the roughness and moisture conditions expected to constrain the range of possible solutions (Mattia et al., 2006). Another approach has been to retrieve or invert roughness parameters calibrated from a first radar scene (using soil moisture ground measurements) and subsequently use those roughness parameters calibrated on a multitemporal series of scenes (Su et al., 1997; Walker et al., 2004; Baghdadi et al., 2002b; 2004; 2006). Lastly, empirical and semi-empirical models have also been proposed to offer alternative expressions for the inversion of surface parameters.

The empirical models are based on experimental scatterometer observations, whereas the semi-empirical models consist of empirical fittings to the predictions of theoretical models. Generally, both types of models are developed to offer algorithms with a wider range of applicability and with improved inversion capabilities, as they provide approximate solutions that often require a single roughness parameter (Oh et al., 1992; Dubois et al., 1995; Oh, 2004) or even none (Chen et al., 1995). Empirical and semi-empirical models have been applied with varied success (Wang et al., 1997; van Oevelen and Hoekman, 1999; Leconte et al., 2004; Walker et al., 2004; D'Urso and Minacapilli, 2006). Adequate results have often been obtained after calibrating the roughness parameters (Leconte et al., 2004; Walker et al., 2004; D'Urso and Minacapilli, 2006); however, the applicability and adequacy of the models to different surface conditions and sensor configurations have not been clearly assessed, and a comparative analysis of different models is required.

In a recent publication, Baghdadi and Zribi (2006) evaluated the IEM and empirical models of Oh et al. (1992) and Dubois et al. (1995) using a large database consisting of C-band synthetic aperture radar (SAR) images (ERS-2, RADARSAT-1, and ASAR) and ground measurements (soil moisture and roughness). The results of this study revealed that the model of Oh et al. correctly simulated the copolarization ratio ($p$) but systematically overestimated the cross-polarization ratio ($q$) and underestimated the backscattering coefficient for HV polarization. On the other hand, the Dubois model faithfully reproduced the radar signal for intermediate roughness conditions and incidence angles $\theta \leq 34°$, whereas the model performance was poor for smooth or rough surfaces and also for small incidence angles. Lastly, the IEM overestimated the backscatter for HH polarized observations, whereas for VV polarization the overestimation was very small. Although the evaluation of Baghdadi and Zribi provided interesting results, further analyses need to be performed to fully assess the performance of these models under varied conditions.

In this paper the empirical models of Oh et al. (1992) and Dubois et al. (1995) and the semi-empirical models of Chen et al. (1995), Shi et al. (1997), and Oh (2004) are studied. The performance of these models is evaluated first analytically by comparing their simulations with those obtained with theoretical models; in this case the sensor configuration considered is close to the optimum configuration for soil moisture inversion (Ulaby et al., 1986; Biftu and Gan, 1999), namely C-band frequency, HH polarization, and 20° incidence angle. The model estimations are then compared with radar observations acquired by RADARSAT-1 over an experimental catchment of Navarre, northern Spain. The aim of the study is to assess the applicability of the models on different conditions often found over agricultural areas.

## Backscattering models

The theoretical models used as a reference and the empirical and semi-empirical models tested are briefly described in this

section. For the sake of simplicity, the complete formulation of the models is not included because they are well defined in the literature.

## Theoretical models

*Integral equation model (IEM)*

The IEM (Fung, 1994) is the theoretical backscattering model with the widest range of applicability. The complete version of the IEM is applicable over a full range of surface roughness and frequency conditions, since it describes both the single and multiple scattering components. However, in most situations the multiple scattering component can be neglected and the single scattering solution provides adequate results (Fung, 1994). In addition, the single scattering solution is less complex and easier to implement. Multiple scattering hardly occurs on surfaces where $ks < 3.0$ and $\gamma < 0.4$, where $k$ is the wavenumber ($cm^{-1}$), $\gamma$ is the surface roughness slope, and $s$ is the standard deviation of the surface height (cm), so these conditions restrict the applicability of the single scattering solution to surfaces with smooth to moderate roughness conditions.

The IEM calculates the backscattering coefficient from a soil surface given the scene acquisition parameters (frequency, incidence angle $\theta$, and polarization), the dielectric constant of the soil surface $\varepsilon$, and its roughness parameters, namely $s$, $l$, and the ACF shape that over natural surfaces can be assumed to be exponential. The model can be inverted to estimate the dielectric constant, and hence the soil moisture, using numerical methods.

*Geometrical optics model (GOM)*

The GOM represents the stationary phase solution of the Kirchhoff models (KM). This solution is based on the assumption that the coherent backscattering term is much smaller than the noncoherent component and thus can be neglected (Ulaby et al., 1986). These circumstances are usually met on rough or very rough conditions occasionally found over natural surfaces. The validity range of the GOM is restricted to the following (Ulaby et al., 1986): $(2ks \cos \theta) > 10$ and $l^2 > 2.76\lambda s$ (where $k$ is expressed in $cm^{-1}$, $\theta$ in degrees, and $s$, $l$, and $\lambda$ in cm). The GOM calculates the backscattering coefficient from a surface given the scene acquisition parameters, $\varepsilon$, and the roughness parameters ($s$, $l$, and ACF shape) of the soil surface.

## Empirical models

The empirical models analyzed in this paper were both developed based on ground-based scatterometer observations acquired under a variety of roughness, moisture, and sensor configurations.

*Empirical model of Oh et al. (1992) (EMO)*

The EMO was based on a set of experimental multipolarized observations acquired at L-, C-, and X-band frequencies and incidence angles ranging from 10° to 70°. The surface roughness and soil moisture conditions of the experimental sites covered the following ranges: $0.1 < ks < 6.0$, $2.6 < kl < 19.7$, and $0.09 < SM < 0.31$ (where $k$ is expressed in $cm^{-1}$, $s$ and $l$ in cm, and SM in $cm^3 \cdot cm^{-3}$). The EMO provides expressions for the copolarization and cross-polarization ratios ($p$ and $q$, respectively) and also for the backscattering coefficients for HH, VV, and HV polarizations. An important advantage of the EMO is that it requires one single roughness parameter ($s$), and hence it can be more easily inverted than other models. Additionally, in cases where multipolarized observations are available, the EMO can be used to invert both the dielectric constant and $s$ with no need for ground measurements.

The EMO does not include the coherent component of the backscattering, so its application is not recommended over smooth surfaces observed at incidence angles below 20°.

*Empirical model of Dubois et al. (1995) (EMD)*

The EMD was based on a set of experimental multipolarized observations similar to those of the EMO, with L-, C-, and X-band frequencies and incidence angles ranging from 10° to 70°. The EMD provides expressions for the calculation of the backscattering coefficient at HH and VV polarizations with the following validity range: $ks \leq 2.5$, $\theta \geq 30$, and $SM < 0.35$ (where $k$ is expressed in $cm^{-1}$, $s$ in cm, $\theta$ in degrees, and SM in $cm^3 \cdot cm^{-3}$). The EMD provided good results when validated against AIRSAR observations (Dubois et al., 1995) and independent applications (Wang et al., 1997; Leconte et al., 2004).

## Semi-empirical models

The practical application of empirical models can be problematic due to the limited validity ranges within which these models can be used. Therefore, some researchers proposed backscattering models empirically fitted to simulations obtained by theoretical models (mainly the IEM), thus circumventing the site dependency of models based on observations. Those models aim at providing simplified solutions to the theoretical algorithms that can be more easily applied and inverted.

*Semi-empirical model of Chen et al. (1995) (SEMC)*

The SEMC is based on the single scattering term of the IEM. It is a multiple regression model fitted to a set of IEM simulations. The SEMC provides an algorithm relating the copolarization ratio of the backscattering coefficient, $\sigma^0_{HH/VV}$, to the soil moisture, observation frequency, and incidence angle. It does not require any roughness parameters because it is based on the assumption that the copolarization ratio is not dependent on the roughness of the observed surface. It is applicable over the following conditions: $0.1 < s < 2.0$, $1.0 < l < 15.0$, $0.10 < SM < 0.40$, $10 < \theta < 50$, and $1 < \text{frequency} < 10$ (where $s$ and $l$ are expressed in cm, SM in $cm^3 \cdot cm^{-3}$, $\theta$ in degrees, and frequency in GHz).

*Semi-empirical model of Shi et al. (1997) (SEMS)*

The SEMS was also derived from a regression analysis of data generated by the single scattering term of the IEM. This

model was developed to provide a straightforward algorithm for application to SAR data. It requires only one roughness parameter, $S_R$, which is a combination of $s$ and the surface power spectrum $W$. It can best be inverted using copolarized observations, since it then yields estimates of both the soil moisture and the roughness parameter. Shi et al. (1997) also provided the empirical coefficients to apply it to VV-polarized observations, but not for the HH polarization. However, if applied to single polarized observations, the roughness parameter needs to be precisely estimated for an accurate soil moisture inversion.

The algorithm was generated using data from only L-band frequencies, whereas the incidence angle and surface parameter ranges considered were broad: $0.2 < s < 3.6$, $2.5 < l < 35.0$, $0.02 < \mathrm{SM} < 0.50$, and $25 < \theta < 70$ (where $s$ and $l$ are expressed in cm, SM in $\mathrm{cm}^3 \cdot \mathrm{cm}^{-3}$, and $\theta$ in degrees).

*Semi-empirical model of Oh (2004) (SEMO)*

The SEMO provides an inversion of the soil moisture from a previous model (Oh et al., 2002), which was based on ground-based scatterometer observations while agreeing with theoretical model simulations (Oh, 2004). To facilitate the inversion, the SEMO introduces a new equation for the cross-polarized ratio that does not depend on the correlation length $l$. Therefore, the model requires only the roughness parameter ($s$) and can be easily inverted using multipolarized observations. The validity conditions of the SEMO cover the following ranges: $0.13 < ks < 3.5$, $0.04 < \mathrm{SM} < 0.29$, and $10 < \theta < 70$ (where $k$ is expressed in $\mathrm{cm}^{-1}$, $s$ in cm, SM in $\mathrm{cm}^3 \cdot \mathrm{cm}^{-3}$, and $\theta$ in degrees). The model was successfully applied to airborne multipolarized SAR observations. Moreover, the accuracy of the results improved when multiple frequency observations were used and their inverted SM and $s$ values averaged.

## Analytical evaluation

The backscattering models selected were first analytically evaluated comparing their simulations with reference estimations predicted by theoretical models. The analytical evaluation was performed in two steps. First, the sensitivity of each model to the main variables influencing the backscatter was analyzed and compared to the behaviour of the IEM. The variables studied were the incidence angle $\theta$, the soil moisture SM, and the standard deviation of surface heights $s$. Next, different scenarios concerning the roughness of the soil surface and the incidence angle were considered and the discrepancy between each model and the reference theoretical model was computed through the root mean square error, rmse (in dB), of the backscatter estimated over a full range of soil moisture conditions.

In the first analysis, the sensor configuration considered corresponded to C-band frequency and HH polarization, which combined with small incidence angles provided an adequate configuration for soil moisture sensing (Ulaby et al., 1986; Biftu and Gan, 1999). First, the sensitivity of the backscatter to the incidence angle was studied assuming average surface roughness and soil moisture conditions, i.e., $s$ = 1.0 cm, $l$ = 6.0 cm, and SM = 0.25 $\mathrm{cm}^3 \cdot \mathrm{cm}^{-3}$ ($\varepsilon \approx 12$), and an incidence angle range from 10° to 50°. Next, the sensitivity of the backscatter to the soil moisture was analyzed considering a moisture range from 0.025 to 0.50 $\mathrm{cm}^3 \cdot \mathrm{cm}^{-3}$ (approximately from $\varepsilon = 3$ to $\varepsilon = 29$), an incidence angle of 30°, and keeping the same average roughness conditions. Lastly, the influence of the roughness parameter $s$ on the backscatter was analyzed considering a range from 0.5 cm to 3.0 cm and assuming average incidence angle ($\theta$ = 30°), soil moisture (SM = 0.25 $\mathrm{cm}^3 \cdot \mathrm{cm}^{-3}$), and correlation length values ($l$ = 6.0 cm).

The reference simulations obtained with the IEM showed that, in the case of the incidence angle, a typical decreasing trend was frequently documented (Ulaby et al., 1986; Fung, 1994; Mancini et al., 1999). The sensitivity of the backscatter to the soil moisture decreased as the soil got wetter. Lastly, the sensitivity of the backscatter to $s$ was more complex, as it first increased up to a certain value after which the backscattering coefficient adopted a decreasing trend.

**Figure 1** summarizes the results of this first analysis. The EMO predicted a decreasing trend as the incidence angle increased, although at low incidence angles the backscatter was severely underestimated (**Figure 1a**). The sensitivity to SM was generally correctly reproduced with the EMO (**Figure 1b**), although an offset was observed. Lastly, the EMO predicted an asymptotical increase in backscatter as $s$ got larger, which was not consistent with the IEM trend (**Figure 1c**).

In the case of the EMD, the decrease in backscatter appeared to be too steep (**Figure 1d**). However, the validity range of the EMD is a priori restricted to $\theta \leq 30°$, and over that range the decreasing trend was similar to that of the IEM. On the other hand, the EMD predicted a higher sensitivity to SM at humid conditions, in contrast to the IEM trend (**Figure 1e**). The influence of $s$ on the backscatter followed an asymptotical increase as in the case of the EMO (**Figure 1f**).

The SEMC calculates the copolarization ratio $\sigma^0_{HH/VV}$, and thus in this case the comparison was made against $\sigma^0_{HH/VV}$ simulations obtained with the IEM (**Figures 1g–1i**). According to the IEM, the copolarization ratio decreased slightly as the incidence angle increased. This tendency to decrease was correctly reproduced by a simplified linear trend on the SEMC curve, although a large offset existed between the SEMC and the IEM curve (**Figure 1g**). The sensitivity of the copolarization ratio to SM was represented by the IEM with a slightly decreasing trend (2 dB on a full soil moisture range), whereas the SEMC predicted a sharp fall (from approximately +20 dB to –12 dB) (**Figure 1h**). Lastly, although the SEMC was based on the assumption that the copolarization ratio was not affected by the roughness of the soil surface, the IEM described an ascending trend in the copolarization ratio as $s$ increased.

The results obtained with the SEMS were compared against IEM simulations for VV polarization. The sensitivity to the incidence angle was correctly reproduced by the SEMS at small and medium incidence angles (**Figure 1j**). At large incidence angles (>45°) an unrealistic sharp fall was predicted by the

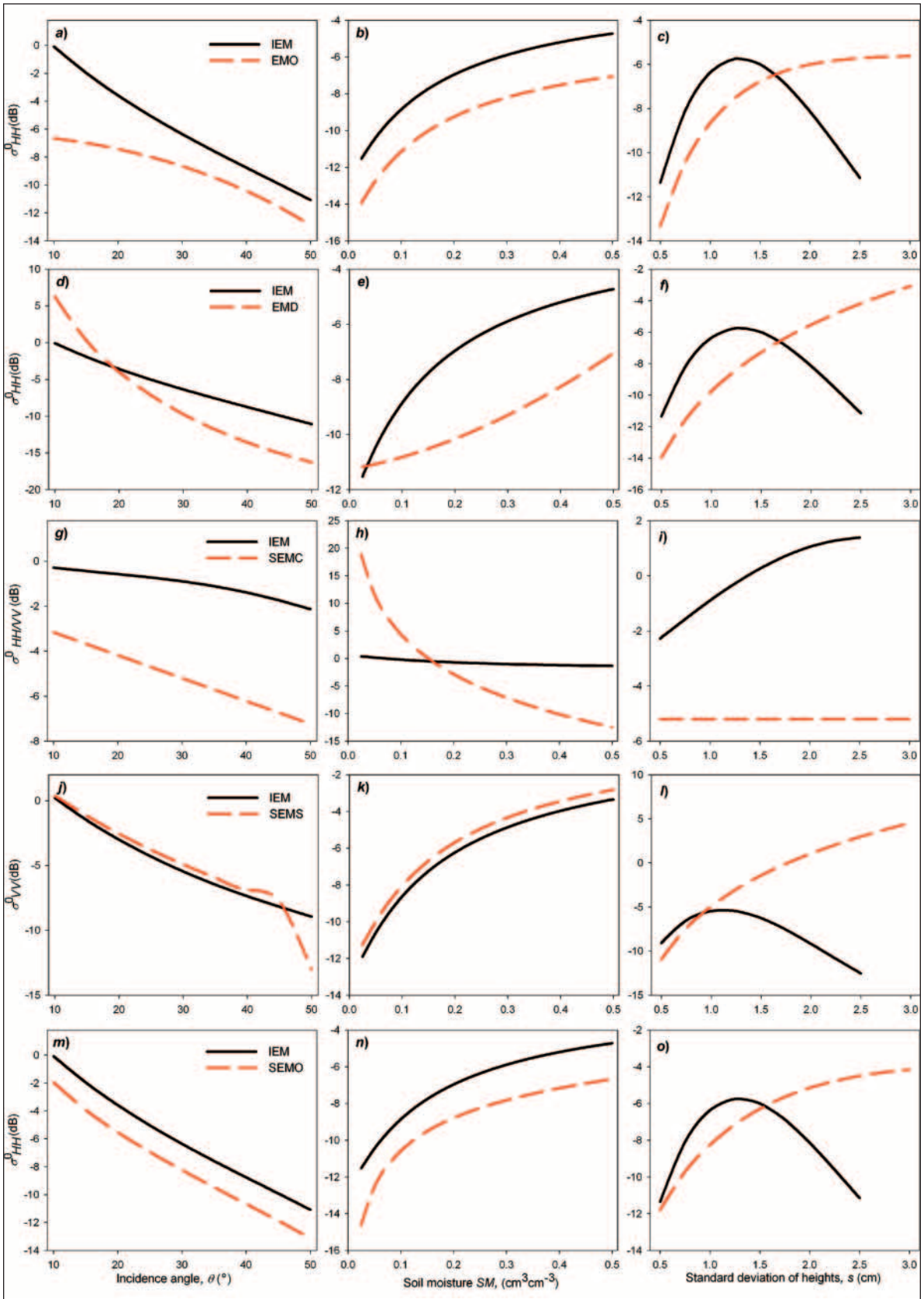


**Figure 1.** Sensitivity of the studied models EMO (a, b, and c), EMD (d, e, and f), SEMC (g, h, and i), SEMS (j, k, and l), and SEMO (m, n, and o) to the incidence angle θ, soil moisture SM, and standard deviation of heights *s* as compared with that of the IEM.

**Table 1.** Root mean square error computed between each model and the reference theoretical model.

| | | Root mean square error (rmse, dB) | | | | |
|---|---|---|---|---|---|---|
| Roughness class | θ (°) | EMO | EMD | SEMC | SEMS | SEMO |
| Smooth ($s$ = 0.7 cm, $l$ = 2.5 cm) | 20 | 4.61 | 1.47 | 8.12 | 1.50 | 2.39 |
| | 40 | 2.20 | 4.41 | 7.49 | 0.36 | 2.10 |
| Medium ($s$ = 1.5 cm, $l$ = 4.0 cm) | 20 | 2.59 | 7.53 | 8.34 | 10.66 | 4.53 |
| | 40 | 1.42 | 3.27 | 8.57 | 5.33 | 1.72 |
| Rough ($s$ = 3.0 cm, $l$ = 7.0 cm) | 20 | 0.52 | 7.61 | 8.60 | 10.22 | 2.41 |
| | 40 | 1.09 | 1.00 | 9.34 | 7.98 | 0.41 |

**Note:** Three roughness classes and two incidence angle (θ) configurations are considered. IEM is used as reference except for the "rough" roughness class where the GOM is used instead.

SEMS. The sensitivity to SM was also adequately described, thus the IEM trend was closely reproduced by the SEMS (**Figure 1k**). On the other hand, the influence of $s$ was described by an increasing asymptotic trend that did not agree with the IEM at medium and rough conditions (**Figure 1l**).

Ultimately, the SEMO correctly described the trend of a decrease in backscatter with an increase in incidence angle over the full incidence angle range (**Figure 1m**). An underestimation of approximately 2 dB was observed. The influence of SM was also correctly described, apart from an offset of 2 dB. The influence of $s$ followed a trend similar to that of the EMO, however, with an asymptotically increasing shape.

The second analytical evaluation consisted of computing the rmse of the backscatter estimated over different scenarios concerning the roughness of the soil surface and the incidence angle. Three roughness conditions were considered which are representative of most of the roughness classes found on agricultural surfaces (Álvarez-Mozos et al., 2006): (*i*) smooth conditions ($s$ = 0.7 cm and $l$ = 2.5 cm) representing seedbed or compacted agricultural surfaces, (*ii*) medium surfaces ($s$ = 1.5 cm and $l$ = 4.0 cm) representative of harrowed or disk-ploughed surfaces, and (*iii*) rough surfaces ($s$ = 3.0 cm and $l$ = 7.0 cm) corresponding to mouldboard-ploughed or deeply harrowed surfaces. For the first two roughness classes, the IEM was used as the reference theoretical backscattering model. The latter was out of the applicability range of the IEM, so the GOM was used as a reference in that case.

Two incidence angle configurations were selected, namely θ = 20° and θ = 40°, which represented the limits of the standard incidence angle range of most SAR sensors, i.e., ENVISAT–ASAR, RADARSAT-1, RADARSAT-2, ALOS–PALSAR, and TERRASAR. The small incidence angle configuration is a priori best suited for soil moisture retrieval. However, some of the models studied are not applicable at small incidence angles.

The results obtained are summarized in **Table 1** and **Figure 2**. The EMO showed a better agreement with reference models over rough conditions with rmse values of 1 dB or less. The agreement was poor at small incidence angles, especially for smooth surfaces. The reason for this lack of agreement can be explained in that under these conditions an important proportion of the backscatter comes from the coherent scattering component, which is not represented in the EMO. Boisvert et al. (1997) also observed an underestimation of the HH backscattering coefficient calculated with the EMO. On the other hand, Baghdadi and Zribi (2006) did not evaluate the HH backscatter simulations of the EMO, but they observed a correct simulation of the copolarization ratio ($p$), an overestimation of the cross-polarization ratio ($q$), and an underestimation of the backscattering coefficient for the HV polarization.

At an incidence angle of 40°, the EMD yielded better results as surfaces became rougher, with rmse values decreasing from 4 dB to 1 dB (**Table 1**; **Figure 2**). Although rmse values were 1.47 dB at 20° and smooth conditions, they were much higher at medium and rough conditions. The applicability of the EMD at low incidence angles is indeed not recommended.

The SEMC yielded rmse values over 7 dB in all cases (**Table 1**; **Figure 2**). The lack of agreement observed could be due to the fact that the SEMC was developed considering roughness parameters corresponding to very smooth surfaces, which are unusual on natural surfaces.

The SEMS provided good agreement with the IEM when applied to smooth surfaces, particularly when observed at large incidence angles (**Table 1**; **Figure 2**). However, at medium and rough surfaces the rmse values increased dramatically, especially at an incidence angle of 20°.

Lastly, the SEMO yielded lower rmse values on the simulations performed at a 40° incidence angle than on those at 20° (**Table 1**; **Figure 2**). In addition, at an incidence angle of 40° the agreement improved as the surface became rougher. On the other hand, at an incidence angle of 20° the agreement was moderate (<2.5 dB) over smooth and rough conditions, whereas it was poor over medium roughness conditions.

# Experimental evaluation

### Research site

The experimental study was carried out over a small agricultural watershed located in the Spanish region of Navarre called La Tejería (**Figure 3**). This watershed is part of the Experimental Agricultural Watershed Network of Navarre

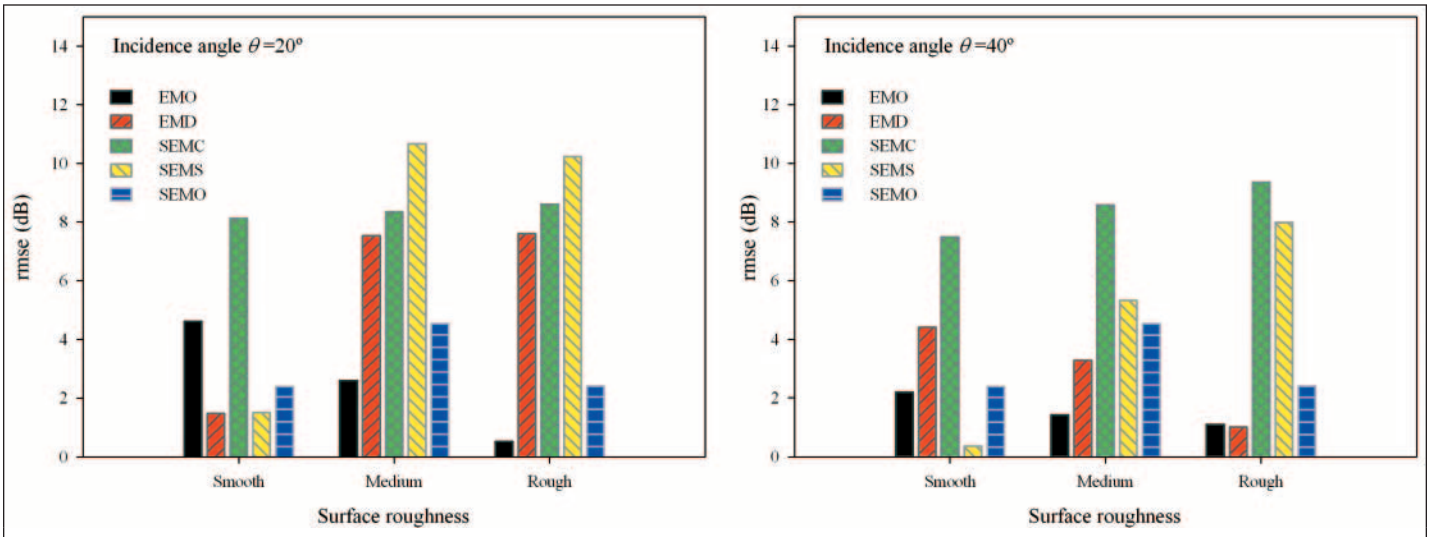


**Figure 2.** Results obtained from the analytical evaluation. Root mean square errors (rmse) calculated between EMO, EMD, SEMC, SEMS, and SEMO predictions and those of the reference models. Two incidence angles and three surface roughness conditions are considered.

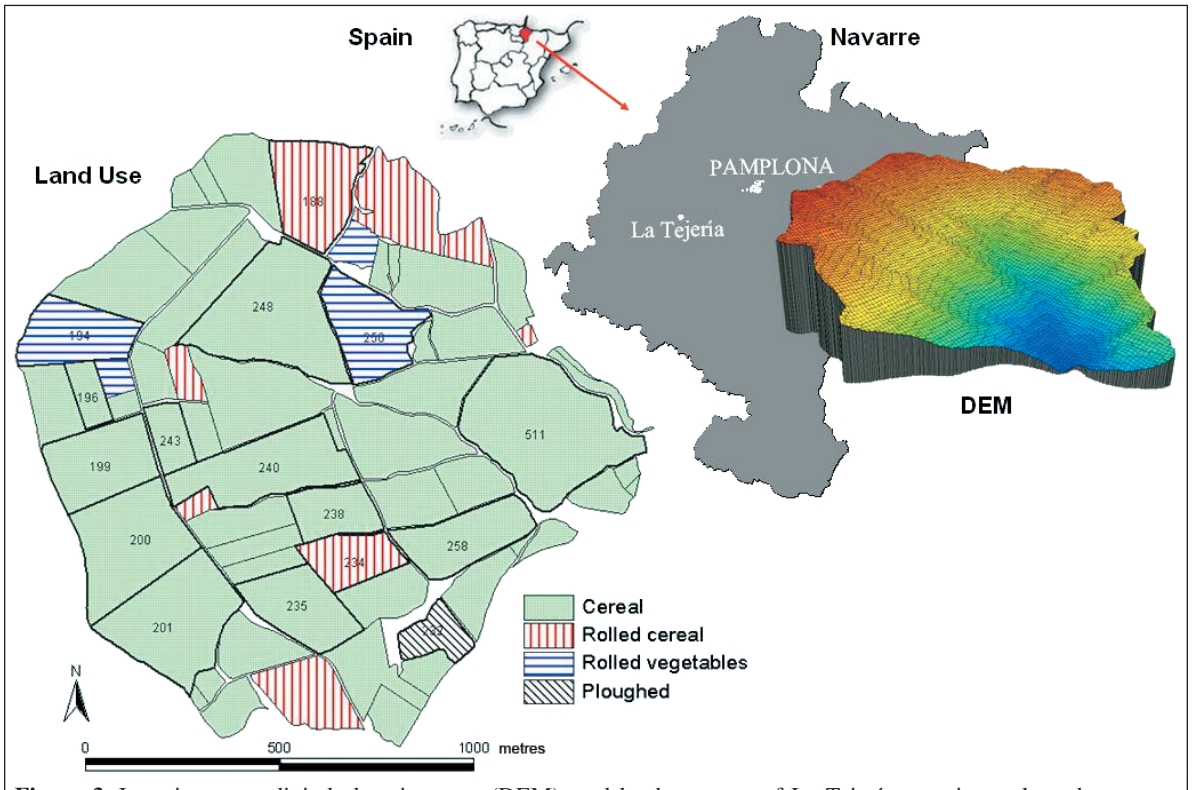


**Figure 3.** Location map, digital elevation map (DEM), and land use map of La Tejería experimental catchment.

created in 1993 (Casalí et al.[2]). The watershed covers approximately 160 ha and has homogeneous slopes of about 12%. The climate is humid submediterranean, and soils have clayey textures and are approximately 1 m thick. The watershed is devoted to agriculture and is almost completely cultivated. During the experimental period (February–April 2003), an emerging cereal crop covered most of the fields of La Tejería watershed, except for one ploughed field and four other fields where vegetable crops had been sown by scattering the seed over previously rolled soils (classified as "rolled

[2] J. Casalí, R. Gastesi, J. Alvarez-Mozos, L.M. De Santisteban, J. Del Valle De Lersundi, M. Goñi, and M.A. Campo. Runoff, erosion and water quality of agricultural watersheds in central Navarre (Spain). *CATENA*. In preparation.

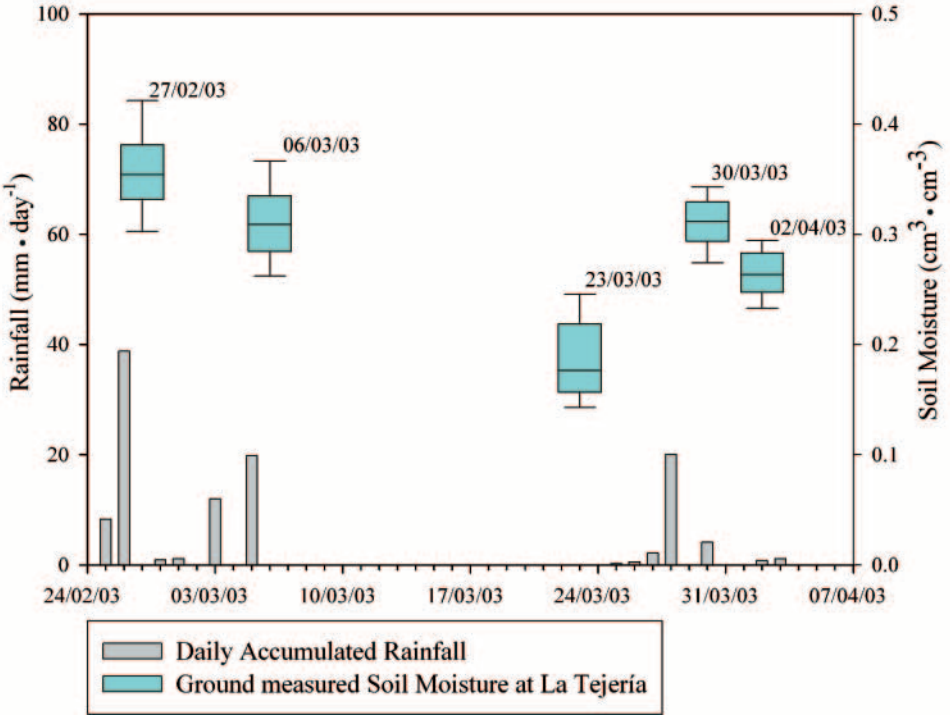


**Figure 4.** Ground measured soil moisture data (in boxplots) at La Tejería watershed during the experimental campaign and the rainfall distribution (bars). Dates are given in day–month–year format.

vegetables"). The cereal fields that had been rolled after sowing, and therefore had a smoother surface, were grouped in a separate crop class called "rolled cereal".

Soil moisture and surface roughness measurements were performed during the experimental period. Surface soil moisture was measured coinciding with image acquisition dates with a calibrated portable time-domain reflectometry (TDR) probe (TRIME-FM3, IMKO GmBH) to provide mean moisture values at 16 control fields and at the catchment scale. The TDR probe consists of three rods with a length of 16 cm. In the present study the probe was inserted with an inclination of 50° to provide the moisture content of the top 10 cm of the soil. Generally, it can be assumed that the soil depth sensed with C-band radar observations varies between 1 and 10 cm depending on the moisture content (Ulaby et al., 1986). Over each control field the soil moisture has been monitored at a minimum of three sampling sites distributed throughout the field, and three TDR readings were acquired at each sampling site. To obtain representative catchment average SM values, a total of 60 sampling sites (three TDR measurements were also acquired at each site) were monitored on each image acquisition date. These sampling sites were selected following a stratified random sampling scheme taking into account the existing crop and soil classification. Average catchment SM values were calculated through a weighted mean. The SM values observed reflected rainfall patterns and ranged approximately from 0.15 to 0.45 $cm^3 \cdot cm^{-3}$ (**Figure 4**).

Surface roughness was measured using a 1 m long needle profiler to provide reference roughness parameters (i.e., $s$ and $l$ values) for each tillage class (**Table 2**). Several profiles were acquired for each tillage class. Profiles were collected parallel and perpendicular to the tillage row direction because no clear row pattern was evident, except for the "ploughed" class where only parallel profiles were processed. Roughness was considered to be invariant in time because no tillage was performed in the experiment period and the intensity of the precipitation events observed was low. The catchment average roughness parameters were $s$ = 1.00 cm and $l$ = 3.47 cm, with standard deviations of 0.13 cm and 2.87 cm, respectively. The catchment average $s$ value was calculated as the weighted average of the different classes, and the average $l$ value was derived from the average autocorrelation function of the different classes.

## Radar scenes

Five RADARSAT-1 SAR-georeferenced fine resolution (SGF) scenes were acquired over the Navarre region during the spring of 2003. The scenes were acquired in a period of approximately 1 month (27 February – 2 April 2003). Beam modes S1 and S2 were selected for their lower incidence angles, on average 23.5° and 27.5°, respectively. The RADARSAT-1 configuration (C-band and HH polarization), at low incidence angles, has proved to be particularly well suited for SM research over cereal

**Table 2.** Measured roughness parameters for each tillage class.

| Class | Total area (ha) | No. of profiles | Standard deviation of the surface height, *s* (cm) | | Surface correlation length, *l* (cm) | |
|---|---|---|---|---|---|---|
| | | | Average | Standard deviation | Average | Standard deviation |
| Rolled vegetables | 10.35 | 16 | 0.47 | 0.09 | 2.44 | 2.84 |
| Rolled cereal | 17.95 | 20 | 0.89 | 0.27 | 3.62 | 3.26 |
| Cereal | 126.27 | 48 | 1.05 | 0.34 | 3.49 | 2.63 |
| Ploughed | 1.77 | 4 | 2.57 | 0.72 | 7.41 | 2.35 |

canopies where vertically polarized waves are more intensively attenuated (Mattia et al., 2003).

Scenes were processed following standard procedures. Calibration was carried out following the approach of Shepherd (2000) and taking into account the topography in the calculation of the local incidence angle (Ulander, 1996). Speckle was reduced applying a 7 × 7 GammaMAP filter (Lopes et al., 1990), and scenes were geocoded following the standard ground control point approach (the accuracy was rmse ≤ 1 pixel) (**Figure 5**). The influence of the emerging cereal cover on the backscattering coefficient was corrected by means of the semi-empirical "water cloud" model (Attema and Ulaby, 1978). For this correction, it was assumed that the cereal canopy only influenced the backscatter by attenuating the radar signal. In addition, the canopy attenuation (loss factor) was assumed to depend only on the canopy moisture content, $M_V$ (in $kg \cdot m^{-2}$), which was estimated using some reference ground measurements and a Landsat-7 enhanced thematic mapper plus (ETM+) derived normalized difference vegetation index (NDVI) image (further details in Álvarez-Mozos et al., 2006). Lastly, field average backscattering values were computed.

## Experimental results

RADARSAT-1 $\sigma^0$ observations were compared against model simulations at the field and catchment scales. The SEMC requires backscattering observations at both HH and VV polarizations, and therefore, given that only RADARSAT-1 HH observations were available, this model could not be tested using experimental data. Additionally, the SEMS could not be applied because this model requires VV-polarized observations or VV- and HH-polarized observations. The empirical coefficients *a* and *b* required for the calculation of the backscattering coefficient $\sigma^0$ at HH polarization have not yet been published. The experimental evaluation thus focused on the EMO, EMD, and SEMO.

The differences between IEM results and RADARSAT-1 observations are discussed first. At the field scale, IEM simulations showed a reasonable agreement with RADARSAT-1 observations (**Figure 6**). The dispersion and discrepancies between observed and estimated backscatter (e.g., **Figure 6a**) can be at least partially attributed to the inherent variability of surface roughness and the difficulties related to its measurement. The consequences of roughness measurement inaccuracies are even more critical on smooth surfaces (**Figures 6b, 6c**) because of the higher sensitivity of the backscatter to the roughness parameters at low *s* and *l* values. The influence of roughness variability is reduced when moving to the catchment scale, where the agreement between IEM results and observations improves.

Most of the fields in La Tejería belonged to the "cereal" tillage class. The backscatter values estimated with the IEM for those fields showed a reasonable agreement with the observations, although an overestimation was observed at low backscatter values (low moisture conditions) (**Figure 6a**). The EMO and EMD consistently underestimated the backscatter. The former predicted a trend similar to that of the IEM but approximately 2–3 dB lower, especially at moist conditions, whereas the latter showed a greater dispersion and normally underestimated the backscattering coefficient by as much as 3–4 dB. On the other hand, the SEMO predictions followed the observations closely, particularly at moist conditions, whereas over dryer situations an overestimation of around 2–3 dB was noticed, similar to that of the IEM (**Figure 6a**).

Rolled cereal fields had a smoother surface. In those fields the IEM forecasted backscatter values 2–4 dB higher than the observed values (**Figure 6b**). The SEMO estimations, however, showed a close agreement with the observations which became slightly worse in dry conditions. As expected, the EMO and EMD underestimated the backscatter values to a greater extent over rolled cereal fields than over cereal fields (**Figure 6b**). This underestimation was also more evident over fields belonging to the class "rolled vegetables", which showed very smooth conditions (**Figure 6c**). In those fields, the IEM simulations also showed a poor agreement with the observations. The large sensitivity of the backscattering coefficient to *s* in smooth conditions is the reason why small inaccuracies in the determination of *s* cause significant errors in the prediction of backscatter.

Lastly, the analysis of the ploughed class was limited because there was only one field belonging to this class. Due to the rougher conditions, the GOM was used instead of the IEM. The GOM predictions followed the observations, although a constant overestimation of around 2 dB was noticed (**Figure 6d**). The EMO showed a behaviour very similar to that of the GOM, as could be expected from the analytical evaluation performed. Conversely, the EMD and SEMO largely overestimated the backscatter over the entire moisture range (**Figure 6d**).

At the catchment scale, models behaved similarly to the case of the cereal fields (**Figure 7**). The IEM and SEMO showed

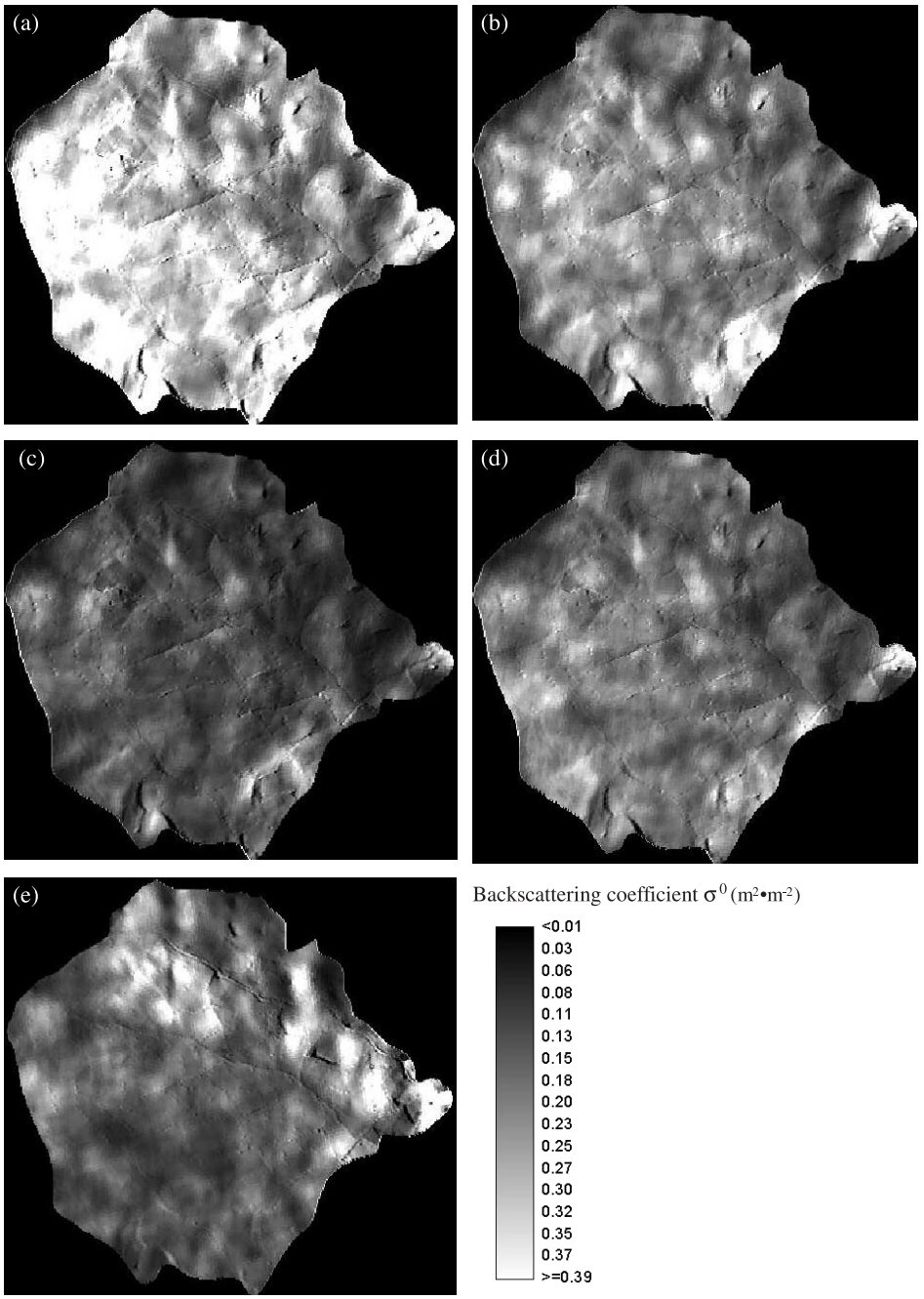


**Figure 5.** RADARSAT-1 scenes acquired over La Tejería experimental catchment. Scenes are already processed and calibrated: (a) 27 February 2003; (b) 6 March 2003; (c) 23 March 2003; (d) 30 March 2003; and (e) 2 April 2003.

close agreement with the observations. The EMO and EMD underestimated the backscattering coefficient by several decibels, particularly in moist conditions.

The results plotted were analyzed computing the root mean square error rmse between the observations and model simulations (**Table 3**). The IEM yielded, on average, the smallest rmse values, although smooth fields showed poorer results (rmse = 2.44 dB in the rolled vegetables class). The SEMO produced accurate results at the field scale, with rmse values of around 1 dB in the cereal and rolled cereal fields, as well as at the catchment scale. The SEMO yielded large errors over very rough conditions (rmse = 4.96 dB), but those results were not very representative because data from only one field with significant roughness were analyzed. The EMO generally underestimated the backscatter, particularly over smooth surfaces and in moist conditions (rmse = 5.54 dB in the rolled vegetables class); at the catchment scale this model produced an rmse of around 2 dB. Lastly, the EMD yielded, on average,

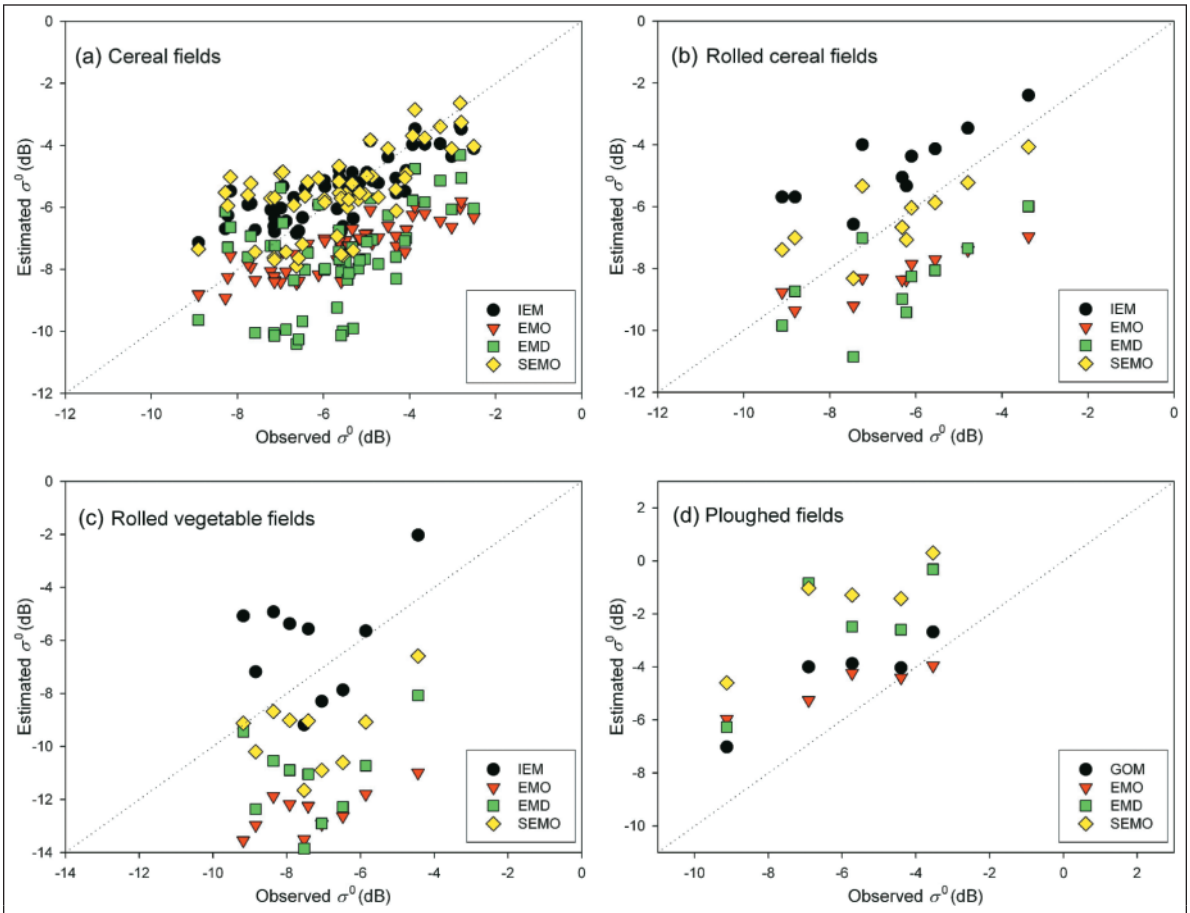


**Figure 6.** Model-estimated $\sigma^0$ values versus RADARSAT-1 observations at the field scale. Fields are plotted grouped according to their tillage class: (a) cereal, (b) rolled cereal, (c) rolled vegetables, and (d) ploughed.

the largest rmse values. In addition, it underestimated the backscatter over the smooth surfaces and overestimated it over the rough surfaces. These results are in agreement with those obtained by Baghdadi and Zribi (2006). Therefore, the use of the EMD at incidence angles below 30° is not recommended.

## Concluding remarks

The present study compared the behaviour of several empirical and semi-empirical backscattering models against theoretical models and RADARSAT-1 observations. The objective of this research was to identify the conditions where each model could best be applied. Both evaluations (analytical and experimental) are complementary and the results normally agree, but some models could not be experimentally evaluated because they were not applicable to the sensor configuration of RADARSAT-1.

The empirical model of Oh et al. (1992) did not show adequate experimental results over fields with smooth and medium roughness conditions, particularly when observed at small incidence angles. Under these conditions, backscatter was underestimated by as much as 5 dB, in particular when backscatter was estimated under wet soil conditions. Conversely, the empirical model of Oh et al. accurately

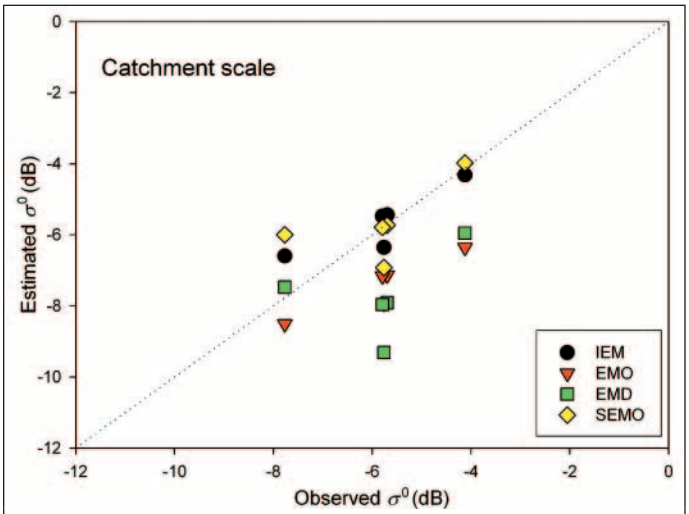


**Figure 7.** Model-estimated $\sigma^0$ values versus RADARSAT-1 observations at the catchment scale.

estimated backscatter for rough surfaces. This finding is in accordance with the results of the analytical evaluation.

The analytical results showed that the empirical model of Dubois et al. (1995) yielded better results at large incidence angles. This finding was corroborated by the experimental

**Table 3.** Root mean square error (rmse) computed between each model and RADARSAT-1 observations.

| Tillage class | IEM (dB) | EMO (dB) | EMD (dB) | SEMO (dB) |
|---|---|---|---|---|
| Cereal | 0.98 | 1.96 | 2.51 | 1.26 |
| Rolled cereal | 2.19 | 2.13 | 2.44 | 1.17 |
| Rolled vegetables | 2.44 | 5.54 | 4.52 | 2.78 |
| Ploughed | 2.08[a] | 1.95 | 4.16 | 4.96 |
| Catchment scale | 0.70 | 1.88 | 2.53 | 1.06 |

**Note:** Results at the field scale are presented grouped according to the tillage class. Results obtained at the catchment scale are also included.
[a]The theoretical model applied to this class was GOM instead of IEM.

evaluation where the Dubois et al. model showed a strong disagreement with RADARSAT-1 observations acquired at low incidence angles. On the other hand, the sensitivity of the backscattering coefficient to soil moisture was not realistically reproduced by this model, since it predicted an increasing sensitivity as the soil moisture content increased, which was contrary to theoretical predictions and experimental evidence.

The semi-empirical model of Chen et al. (1995) did not compare satisfactorily with theoretical models. The analytical evaluation showed large discrepancies over different incidence angles and roughness conditions. Furthermore, the main assumption underlying the model (the independency of the copolarization ratio $\sigma^0_{HH/VV}$ on surface roughness) did not hold for the conditions considered.

The analytical evaluation of the semi-empirical model of Shi et al. (1997) showed good results over smooth conditions and incidence angles up to 40°. The results were poor over medium and rough conditions. However, if applied to observations acquired in L-band frequency (or lower), the applicable roughness conditions broaden significantly. In addition, the possibility of simplifying the roughness parameter if copolarized observations are available is attractive, and this could be done in the case of ALOS/PALSAR observations (L-band, multipolarized observations).

Lastly, the semi-empirical model of Oh (2004) also provided accurate results. The analytical evaluation showed that at large incidence angles (40°) the results improved as the surface became rougher. In addition, over smooth surfaces and low incidence angles the results were adequate and compared satisfactorily with experimental observations on conventional cereal fields. This model has the additional advantage of requiring only one roughness parameter, facilitating the inversion of soil moisture.

## Acknowledgments

The authors would like to thank the reviewers for their valuable comments. This study was partly funded by the Spanish Government National Scientific Research, Development and Technological Innovation Plan, project code REN2003-03028/HID, and the Canadian Space Agency Data for Research Use program, project DRU-10-02.

## References

Altese, E., Bolognani, O., Mancini, M., and Troch, P.A. 1996. Retrieving soil moisture over bare soil from ERS-1 synthetic aperture radar data: sensitivity analysis based on a theoretical surface scattering model and field data. *Water Resources Research*, Vol. 32, No. 3, pp. 653–661.

Álvarez-Mozos, J., Casali, J., Gonzalez-Audicana, M., and Verhoest, N.E.C. 2005. Correlation between ground measured soil moisture and RADARSAT-1 derived backscattering coefficient over an agricultural catchment of Navarre (north of Spain). *Biosystems Engineering*, Vol. 92, No. 1, pp. 119–133.

Álvarez-Mozos, J., Casali, J., Gonzalez-Audicana, M., and Verhoest, N.E.C. 2006. Assessment of the operational applicability of RADARSAT-1 data for surface soil moisture estimation. *IEEE Transactions on Geoscience and Remote Sensing*, Vol. 44, No. 4, pp. 913–924.

Attema, E.W.P., and Ulaby, F.T. 1978. Vegetation modeled as a water cloud. *Radio Science*, Vol. 13, No. 2, pp. 357–364.

Baghdadi, N., and Zribi, M. 2006. Evaluation of radar backscatter models IEM, OH and Dubois using experimental observations. *International Journal of Remote Sensing*, Vol. 27, No. 18, pp. 3831–3852.

Baghdadi, N., Gaultier, S., and King, C. 2002a. Retrieving surface roughness and soil moisture from synthetic aperture radar (SAR) data using neural networks. *Canadian Journal of Remote Sensing*, Vol. 28, No. 5, pp. 701–711.

Baghdadi, N., King, C., Chanzy, A., and Wigneron, J.P. 2002b. An empirical calibration of the integral equation model based on SAR data, soil moisture and surface roughness measurement over bare soils. *International Journal of Remote Sensing*, Vol. 23, No. 20, pp. 4325–4340.

Baghdadi, N., Gherboudj, I., Zribi, M., Sahebi, M., King, C., and Bonn, F. 2004. Semi-empirical calibration of the IEM backscattering model using radar images and moisture and roughness field measurements. *International Journal of Remote Sensing*, Vol. 25, No. 18, pp. 3593–3623.

Baghdadi, N., Holah, N., and Zribi, M. 2006. Calibration of the integral equation model for SAR data in C-band and HH and VV polarizations. *International Journal of Remote Sensing*, Vol. 27, No. 4, pp. 805–816.

Biftu, G.F., and Gan, T.Y. 1999. Retrieving near-surface soil moisture from RADARSAT SAR data. *Water Resources Research*, Vol. 35, No. 5, pp. 1569–1579.

Bindlish, R., and Barros, A.P. 2000. Multifrequency soil moisture inversion from SAR measurements with the use of IEM. *Remote Sensing of Environment*, Vol. 71, pp. 67–88.

Boisvert, J.B., Gwyn, Q.H., Chanza, A., Major, D.J., Brisco, B., and Brown, R.J. 1997. Effect of surface soil moisture gradients on modelling radar backscattering from bare fields. *International Journal of Remote Sensing*, Vol. 18, No. 1, pp. 153–170.

Chen, K.S., Yen, S.K., and Huang, W.P. 1995. A simple-model for retrieving bare soil-moisture from radar-scattering coefficients. *Remote Sensing of Environment*, Vol. 54, pp. 121–126.

Davidson, M.W.J., Le Toan, T., Mattia, F., Satalino, G., Manninen, T., and Borgeaud, M. 2000. On the characterization of agricultural soil roughness for radar remote sensing studies. *IEEE Transactions on Geoscience and Remote Sensing*, Vol. 38, No. 2, pp. 630–640.

Du, Y., Ulaby, F.T., and Dobson, M.C. 2000. Sensitivity to soil moisture by active and passive microwave sensors. *IEEE Transactions on Geoscience and Remote Sensing*, Vol. 38, No. 1, pp. 105–114.

Dubois, P.C., Van Zyl, J., and Engman, T. 1995. Measuring soil-moisture with imaging radars. *IEEE Transactions on Geoscience and Remote Sensing*, Vol. 33, No. 4, pp. 915–926.

D'Urso, G., and Minacapilli, M. 2006. A semi-empirical approach for surface soil water content estimation from radar data without a-priori information on surface roughness. *Journal of Hydrology*, Vol. 321, pp. 297–310.

Fung, A.K. 1994. *Microwave scattering and emission models and their applications*. Artech House, Norwood, Mass.

Glenn, N.F., and Carr, J.R. 2004. Establishing a relationship between soil moisture and RADARSAT-1 SAR data obtained over the Great Basin, Nevada, USA. *Canadian Journal of Remote Sensing*, Vol. 30, No. 2, pp. 176–181.

Leconte, R., Brissette, F., Galarneau, M., and Rousselle, J. 2004. Mapping near-surface soil moisture with RADARSAT-1 synthetic aperture radar data. *Water Resources Research*, Vol. 40, No. 1, W01515, doi:10.1029/2003WR002312.

Loew, A., and Mauser, W. 2006. A semiempirical surface backscattering model for bare soil surfaces based on a generalized power law spectrum approach. *IEEE Transactions on Geoscience and Remote Sensing*, Vol. 44, No. 4, pp. 1022–1035.

Lopes, A., Touzi, R., and Nezry, E. 1990. Adaptive speckle filters and scene heterogeneity. *IEEE Transactions on Geoscience and Remote Sensing*, Vol. 28, No. 6, pp. 992–1000.

Macelloni, G., Nesti, G., Pampaloni, P., Sigismondi, S., Tarchi, D., and Lolli, S. 2000. Experimental validation of surface scattering and emission models. *IEEE Transactions on Geoscience and Remote Sensing*, Vol. 38, No. 1, pp. 459–469.

Mancini, M., Hoeben, R., and Troch, P.A. 1999. Multifrequency radar observations of bare surface soil moisture content: a laboratory experiment. *Water Resources Research*, Vol. 35, No. 6, pp. 1827–1838.

Mattia, F., Le Toan, T., Picard, G., Posa, F.I., D'Alessio, A., Notarnicola, C., Gatti, A.M., Rinaldi, M., Satalino, G., and Pasquariello, G. 2003. Multitemporal C-Band radar measurements on wheat fields. *IEEE Transactions on Geoscience and Remote Sensing*, Vol. 41, No. 7, pp. 1551–1560.

Mattia, F., Satalino, G., Dente, L., and Pasquariello, G. 2006. Using a priori information to improve soil moisture retrieval from ENVISAT ASAR AP data in semiarid regions. *IEEE Transactions on Geoscience and Remote Sensing*, Vol. 44, No. 4, pp. 900–912.

McNairn, H., and Brisco, B. 2004. The application of C-band polarimetric SAR for agriculture: a review. *Canadian Journal of Remote Sensing*, Vol. 30, No. 3, pp. 525–542.

Moran, M.S., Peters-Lidard, C.D., Watts, J.M., and McElroy, S. 2004. Estimating soil moisture at the watershed scale with satellite-based radar and land surface models. *Canadian Journal of Remote Sensing*, Vol. 30, No. 5, pp. 805–826.

Oh, Y. 2004. Quantitative retrieval of soil moisture content and surface roughness from multipolarized radar observations of bare soil surfaces. *IEEE Transactions on Geoscience and Remote Sensing*, Vol. 42, No. 3, pp. 596–601.

Oh, Y., and Kay, Y.C. 1998. Condition for precise measurement of soil surface roughness. *IEEE Transactions on Geoscience and Remote Sensing*, Vol. 36, No. 2, pp. 691–695.

Oh, Y., Sarabandi, K., and Ulaby, F.T. 1992. An empirical-model and an inversion technique for radar scattering from bare soil surfaces. *IEEE Transactions on Geoscience and Remote Sensing*, Vol. 30, No. 2, pp. 370–381.

Oh, Y., Sarabandi, K., and Ulaby, F.T. 2002. Semi-empirical model of the ensemble-averaged differential Mueller matrix for microwave backscattering from bare soil surfaces. *IEEE Transactions on Geoscience and Remote Sensing*, Vol. 40, No. 6, pp. 1348–1355.

Sahebi, M.R., Angles, J., and Bonn, F. 2002. A comparison of multi-polarization and multi-angular approaches for estimating bare soil surface roughness from spaceborne radar data. *Canadian Journal of Remote Sensing*, Vol. 28, No. 5, pp. 641–652.

Sano, E.E., Moran, M.S., Huete, A.R., and Miura, F. 1998. C- and multiangle Ku-band synthetic aperture radar data for bare soil moisture estimation in agricultural areas. *Remote Sensing of Environment*, Vol. 64, pp. 77–90.

Satalino, G., Mattia, F., Davidson, M.W.J., Le Toan, T., Pasquariello, G., and Borgeaud, M. 2002. On current limits of soil moisture retrieval from ERS-SAR data. *IEEE Transactions on Geoscience and Remote Sensing*, Vol. 40, No. 11, pp. 2438–2447.

Schmugge, T.J., Kustas, W.P., Ritchie, J.C., Jackson, T.J., and Rango, A. 2002. Remote sensing in hydrology. *Advances in Water Resources*, Vol. 25, pp. 1367–1385.

Shepherd, N. 2000. *Extraction of beta nought and sigma nought from RADARSAT CDPF products*. Altrix Systems, Ottawa, Ont. Technical Report.

Shi, J.C., Wang, J., Hsu, A.Y., O'Neill, P.E., and Engman, E.T. 1997. Estimation of bare surface soil moisture and surface roughness parameter using L-Band SAR image data. *IEEE Transactions on Geoscience and Remote Sensing*, Vol. 35, No. 5, pp. 1254–1266.

Su, Z., Troch, P.A., and De Troch, F.P. 1997. Remote sensing of bare surface soil moisture using EMAC/ESAR data. *International Journal of Remote Sensing*, Vol. 18, No. 10, pp. 2105–2124.

Ulaby, F.T., Moore, R.K., and Fung, A.K. 1986. *Microwave remote sensing: active and passive. Volume III: from theory to applications*. Artech House, Norwood, Mass.

Ulander, L. 1996. Radiometric slope correction of synthetic aperture radar images. *IEEE Transactions on Geoscience and Remote Sensing*, Vol. 34, No. 5, pp. 1115–1122.

van Oevelen, P.J., and Hoekman, D.H. 1999. Radar backscatter inversion techniques for estimation of surface soil moisture: EFEDA-Spain and HAPEX-Sahel case studies. *IEEE Transactions on Geoscience and Remote Sensing*, Vol. 37, No. 1, pp. 113–123.

Walker, J.P., Houser, P.R., and Willgoose, G.R. 2004. Active microwave remote sensing for soil moisture measurement: a field evaluation using ERS-2. *Hydrological Processes*, Vol. 18, pp. 1975–1997.

Wang, J.R., Hsu, A., Shi, J.C., O'Neill, P.E., and Engman, E.T. 1997. A comparison of soil moisture retrieval models using SIR-C measurements over the Little Washita River watershed. *Remote Sensing of Environment*, Vol. 59, pp. 308–320.

Wickel, A.J., Jackson, T.J., and Wood, E.F. 2001. Multitemporal monitoring of soil moisture with RADARSAT SAR during the 1997 Southern Great Plains hydrology experiment. *International Journal of Remote Sensing*, Vol. 22, No. 8, pp. 1571–1583.

Wilson, D.J., Western, A.W., and Grayson, R.B. 2004. Identifying and quantifying sources of variability in temporal and spatial soil moisture observations. *Water Resources Research*, Vol. 40, W02507, doi:10.1029/2003WR002306.